



Marieke M. Hoog Antink, Tim Sewczyk, Stephen Kroll, Pál Árki, Sascha Beutel, Kurosch Rezwan, Michael Maas

Proteolytic ceramic capillary membranes for the production of peptides under flow

Journal Article as: peer-reviewed accepted version (Postprint)

DOI of this document* (secondary publication): <https://doi.org/10.26092/elib/2492>

Publication date of this document: 28/09/2023

* for better findability or for reliable citation

Recommended Citation (primary publication/Version of Record) incl. DOI:

Marieke M. Hoog Antink, Tim Sewczyk, Stephen Kroll, Pál Árki, Sascha Beutel, Kurosch Rezwan, Michael Maas, Proteolytic ceramic capillary membranes for the production of peptides under flow, Biochemical Engineering Journal, Volume 147, 2019, Pages 89-99, ISSN 1369-703X, <https://doi.org/10.1016/j.bej.2019.04.005>

Please note that the version of this document may differ from the final published version (Version of Record/primary publication) in terms of copy-editing, pagination, publication date and DOI. Please cite the version that you actually used. Before citing, you are also advised to check the publisher's website for any subsequent corrections or retractions (see also <https://retractionwatch.com/>).

This document is made available under a Creative Commons licence.

The license information is available online: <https://creativecommons.org/licenses/by-nc-nd/4.0/>

Take down policy

If you believe that this document or any material on this site infringes copyright, please contact publizieren@suub.uni-bremen.de with full details and we will remove access to the material.

Regular article

Proteolytic ceramic capillary membranes for the production of peptides under flow

Marieke M. Hoog Antink^a, Tim Sewczyk^b, Stephen Kroll^{a,c}, Pál Árki^d, Sascha Beutel^b, Kurosch Rezwan^{a,e}, Michael Maas^{a,e,*}

^aAdvanced Ceramics, University of Bremen, Am Biologischen Garten 2, 28359 Bremen, Germany

^bInstitute for Technical Chemistry, Leibniz University Hannover, Callinstraße 5, 30167 Hannover, Germany

^cIfBB – Institute for Bioplastics and Biocomposites, University of Applied Sciences and Arts, Heisterbergallee 10A, 30453 Hannover, Germany

^dInstitute of Electronic and Sensor Materials, Technische Universität Bergakademie Freiberg, Gustav-Zeuner Str. 3, 09559 Freiberg, Germany

^eMAPEX – Centre for Materials and Processes, University of Bremen, 28359 Bremen, Germany

HIGHLIGHTS

- Casein was hydrolyzed under flow conditions using proteolytic ceramic membranes.
- Silanization affected enzyme loading and proteolytic performance.
- Peptide production can be tailored by variation of surface functionalization.

ARTICLE INFO

Keywords:

Membrane bioreactor
Enzyme immobilization
Subtilisin A
Bioactive peptides
Casein digestion
Surface functionalization

ABSTRACT

In this study, we investigate the effect of membrane surface functionalization on the immobilization of the protease subtilisin A and its performance in the production of peptides from the model protein casein under flow. The surface of tubular ceramic membranes was silanized to yield carboxylated and aminated supports for enzyme immobilization via non-covalent and carbodiimide activated binding. The protease density correlated with electrostatic interactions between the positively charged enzyme and the supports, with the highest enzyme density reached on negatively charged, carboxylated membranes (0.019 molecules/nm², noncovalent approach). Enzyme leaching was reduced by covalent binding of protease to carboxylated supports (5% leached) and slightly improved by binding to aminated membranes (46%) over non-covalent binding to unfunctionalized reference capillaries (66%). Regarding carbodiimide activated immobilization, protease on unfunctionalized and aminated supports exhibited a significantly larger specific activity (0.99 μmol/min/mg) than enzymes on carboxylated surfaces (0.15 μmol/min/mg), which suggests preferred enzyme orientation. In protein hydrolysis, these differences in surface-enzyme interactions were reflected by variations in peptide composition and degree of hydrolysis. Accordingly, we demonstrate that surface functionalization critically determines the surface properties of protease support materials for the production of peptides under flow and allows tailoring the performance of proteolytic capillary membranes.

1. Introduction

Bioactive peptides are a potent pool of novel active agents for pharmacotherapy, functional foods and cosmetics [1] with positive influence on the human metabolism [2], including antithrombic, anti-hypertensive, immunomodulatory and antioxidant effects [3]. They are most commonly produced by enzymatic protein hydrolysis (proteolysis) [4,5]. The production of bioactive peptides can be improved over

conventional batch hydrolysis by using immobilized enzymes, which are made insoluble [6], rather than free enzymes [4]. As a result of immobilization, enzyme handling and separation of enzymes from the product is simplified and enzyme reusability and recovery is facilitated [6–8]. Thus, further reactor geometries can be employed and reactions can be controlled more easily [7–9]. Additionally, due to increased rigidity and fixation, immobilized enzymes often exhibit an increased stability against structural changes under non-physiological pH,

* Corresponding author at: Advanced Ceramics, University of Bremen, Am Biologischen Garten 2, 28359 Bremen, Germany.

E-mail address: michael.maas@uni-bremen.de (M. Maas).

<https://doi.org/10.1016/j.bej.2019.04.005>

Received 16 October 2018; Received in revised form 27 March 2019; Accepted 6 April 2019

Available online 07 April 2019

extreme temperature conditions and in organic solvents, as well as against aggregation and autolysis [6–11]. When working with proteases, prevention of autolysis is particularly important, since these enzymes are able to use other enzyme molecules as substrate [6]. However, upon immobilization, enzyme activity is oftentimes reduced by denaturation, loss of enzyme motility, non-optimum enzyme orientation (blockage of the active site) or limitations in mass transfer [6,7,9,10,12]. Especially with regard to large substrates, proper enzyme orientation and reachability of the enzyme are crucial for effective catalysis [6,9]. On the other hand, immobilization-induced enzyme conformational changes can also be used to specifically alter enzyme specificity and selectivity, enzyme activity and inhibition mechanisms [6,9,13]. Appropriate immobilization protocols should increase the overall enzyme productivity through enhanced stability and reusability [7,8,10,12].

There are several immobilization techniques available, which can be classified into support binding, entrapment and cross-linking methods [7,8,10,14]. Carrier-based immobilization can be achieved by physical, ionic or covalent binding to the support [7,10,14]. Using support binding, the properties of the immobilized enzyme will be strongly dependent on the nature of the carrier, the immobilization protocol and its specific conditions [13]. While non-covalent immobilization is caused by comparatively weak electrostatic, hydrophobic or Van der Waal's interactions, covalent binding of enzymes results in a stable linkage between support material and enzyme that prevents enzyme leaching [7,10,14]. Additionally, an increase in enzyme stability might be achieved by multipoint covalent attachment [9,13]. Among covalent immobilization strategies, amide bond formation between amino and carboxyl groups via carbodiimide chemistry is well-established due to the ubiquity of both these functional groups in biomolecules such as enzymes [15]. In bioconjugation, a combination of EDC (1-ethyl-3-(3-dimethylaminopropyl) carbodiimide hydrochloride) and NHS (*N*-hydroxysulfosuccinimide) can be used to form reactive ester intermediates with surface carboxyl groups [15]. These activated carboxylates more readily undergo reactions with available amino groups to form stable amide bonds [15].

Supports for enzyme immobilization are based on various materials, such as organic polymers as well as inorganic materials, like metal oxides, minerals and carbon materials [14,16]. Oxidic, ceramic support materials have the advantage of high resistance against harsh chemical and thermal conditions as well as good mechanical properties [12,16]. Their surfaces are characterized by oxygen atoms with unsaturated bonds, which can be activated by wet-chemical and/or physical processes to form surface hydroxyl groups that enable facile attachment of linker molecules [12,16,17]. Ceramics can be shaped into various geometries with complex and tailorable pore structures and high surface areas suited for high immobilization capacities [12,16]. Using enzymatic membrane reactors, biocatalyzed reactions of both free or immobilized enzymes can be combined with separation processes to increase efficiency and reduce purification costs [10,12,18]. In peptide production, the costs of down-stream separation and purification contribute up to 70% to the overall capital and operating costs [19], i.e. control of product composition is of utmost importance [10]. In case of immobilized enzymes on porous ceramic membranes, contact between substrate and catalyst can be forced by convective flow, facilitating control on both the reaction and the product while enabling high-throughput processing of concentrated feed solutions [12].

Membrane reactors with immobilized enzymes have been used to investigate the behavior of specific enzymes under varying process conditions [12]. Besides substrate flow rate [20,21], temperature [22–25] and pH [23–25], the influence of the support's porous properties on enzyme performance has been studied [26]. In the context of bacteria filtration, Kroll et al. e.g. observed a higher specific activity and smaller wash-out of covalently immobilized anti-bacterial glycoside hydrolase on functionalized ceramic membranes over unspecifically bound enzyme at different applied flow rates [20]. Using

proteolytic ceramic capillaries, Sewczyk et al. showed that a decrease in substrate flow resulted in an increase in residence time and the generation of smaller protein-derived fragments [21]. De Cazes et al. described an intensified degradation of antibiotics by an oxidase-modified ceramic membrane with increased temperature and an improved performance of enzymes immobilized in gelatin compared to free enzyme [22]. In addition to temperature, Bayramoğlu et al. observed that while the overall pH optimum of starch-degrading enzymes was not changed by immobilization, enzymes linked to polymeric membranes exhibited a higher activity over a broader pH range than the free counterpart [23]. In a study by Hou et al., the influence of the polymeric support's mean pore size and ceramic nanoparticle coatings on the performance of oxidase-modified membranes in micropollutant removal was shown [26]. Although this study related the enzyme amount and activity to the loading of the membrane with ceramic particles, specific effects of the coating on chemical surface properties were not investigated.

To overcome the challenge of producing membrane reactor systems with stably immobilized enzymes, while maintaining high levels of specific enzyme activity, it was our goal to study the influence of membrane surface functionalization on the performance of immobilized enzymes in the hydrolysis of proteins under flow. With our set-up, it was possible to evaluate the role of surface modification on protease immobilization and thus peptide production to possibly improve the efficiency of proteolytic enzymatic membrane reactors in future applications. We utilized macroporous ceramic capillary membranes made of yttria stabilized zirconia (YSZ) as immobilization supports. The membranes were functionalized with the aminosilane (3-aminopropyl) triethoxysilane (APTES) and the carboxysilane 3-(triethoxysilyl)propylsuccinic anhydride (TESPSA), respectively, in order to study the effect of the surface chemistry on enzyme immobilization, specific enzyme activity and the produced peptide spectrum. By keeping all other material and process parameters unchanged, the impact of surface chemistry could be studied directly. As model protease and protein we chose the well-characterized enzyme subtilisin A and equally well-established substrate casein.

2. Materials and methods

2.1. Materials

All chemicals were used as received without further purification. 3-(triethoxysilyl)propylsuccinic anhydride (TESPSA, product no. AB 128800) and Wirosil® doubling silicone (product no. 52001) were purchased from abcr and BEGO, Germany, respectively. 2-(*N*-morpholino)-ethane sulphonic acid monohydrate (MES, product no. 6066) and beeswax (white, product no. 5825, Carl Roth, Germany) were acquired from Carl Roth, Germany. Alcalase® 2.5 L (subtilisin A, product no. 06-3112) was provided by Novozyme, Denmark. The properties of subtilisin A are summarized in Table S1.1 of the supplementary material. (3-aminopropyl)triethoxysilane (APTES, product no. A3648), Boc-Ala-ONp (Boc-L-alanine 4-nitrophenyl ester, product no. 15052), casein from bovine milk (product no. C7078), HPLC peptide standard mixture (product no. H2016), *N*-hydroxysuccinimide (NHS, product no. 56480), 4-nitrophenol (product no. 1048), Orange II sodium salt (product no. 75370), Pefabloc® SC (product no. PEFBSC-RO), stearic acid (product no. 175366, formerly Aldrich, Germany), thionin acetate salt (product no. 861340) and tris(hydroxymethyl)aminomethane (TRIS, product no. 154563, formerly Aldrich, Germany) were obtained from Sigma Aldrich, Germany. 1-ethyl-3-(3-dimethylaminopropyl)carbodiimide hydrochloride (EDC, product no. 22980), the Pierce® detergent compatible Bradford assay kit (product no. 23246) and the Pierce® microplate BCA protein assay kit (reducing agent compatible, product no. 23252) were purchased from Thermo Scientific™, Germany. YSZ powder TZ-3Y-E was acquired from Tosoh, Japan. Ultrapure type 1 water (ddH₂O, resistivity > 18.2 MΩ·cm at 25 °C, TOC < 5 ppb), acetonitrile (product no. 2653, Chemsolute, Germany), ethanol absolute

(product no. 20821, VWR Chemicals, Germany), decane (product no. D901, Honeywell, Germany) and *n*-hexane (product no. 24577, VWR Chemicals, Germany) were used as solvents. The casein substrate solutions for digestion experiments were prepared similar to [21] to a stock solution with a concentration of 0.5 g/L in 100 mM TRIS buffer (pH 7.8). The size of molecules was estimated with the open-source molecular builder and visualization tool Avogadro (Version 1.1.1.) [27].

2.2. Fabrication, functionalization and characterization of porous ceramic capillaries

As supports for enzyme immobilization, tubular YSZ membranes were prepared by extrusion following the processing route described by Kroll et al. [28]. In short, a ceramic dispersion was prepared by mixing of 300 g of YSZ, 40 g of decane, 3 g of stearic acid, 28 g of bees wax and 45 mL of hexane. The extrusion paste was deagglomerated by ultrasonication for 5 min and homogenized by high speed stirring for 35 min at 80 °C. The resulting dispersion was filled into the vessel of a custom designed extruder at the Advanced Ceramics group, University of Bremen, Germany, and tempered to 40 °C. Green ceramic capillaries were prepared by pressing the ceramic paste through an extrusion die of 1.6 mm diameter with a pin of 1.0 mm diameter at a speed of 30 cm/min. Prior to sintering at 1050 °C for 2 h, the green capillaries were dried for 7 d at 21 °C.

The efficiency of different types of oxidative ceramic surface activation was evaluated with respect to subsequent silanization with the goal to increase the number of reactive hydroxy groups at the support surface. The influence of hydroxylation via O₂ plasma, a strong acid and hydrothermal hydroxylation in steam atmosphere was compared against an untreated reference. Since the hydrothermal process resulted in the highest amount of functional groups (see Figure S2.1 in the supplementary material), this activation route is detailed in the following. The procedures for O₂ plasma and wet chemical acidic activation are described in the supplementary material (S2). For hydrothermal hydroxylation, tubular membranes of 50 mm length were placed inside an autoclave (Systec™ VX-100, Systec, Germany) and treated for 20 min at a temperature of 121 °C in steam atmosphere of 2 bar (0.2 MPa) pressure. Drying was carried out at 70 °C for 24 h. In the next step, silane molecules were attached to the hydroxylated surface to serve as linkers for enzyme immobilization (Fig. 1B). Analogous to Bartels et al., the oxidatively activated capillary pieces were incubated in aqueous silane solutions of either APTES or TESPSA with concentrations of 0.2 M in ddH₂O [29]. For each 30 cm of capillary material, 10 mL of solution were used. Silanization took place under constant shaking at 150 rpm and a temperature of 65 °C for 24 h. After

incubation, the capillaries were washed with ddH₂O to remove any excess silane until the washing solution retained a neutral pH. Finally, the capillaries were dried at 70 °C for 24 h.

Both unfunctionalized and sintered capillaries were analyzed concerning their microstructure, their porous properties, specific surface area and their biaxial bending strength. Open porosity, mean pore window size and pore size distribution was investigated with Hg intrusion porosimetry, the specific surface area was evaluated by nitrogen adsorption and the biaxial bending strength was investigated using three point bending tests. Scanning electron microscopy (SEM) was applied to image the porous microstructure. The details on these characterization techniques are given in the supplementary material (S3).

To evaluate the success of functionalization, the surface chemistry of the capillary membranes was characterized quantitatively using photometric assays as well as qualitatively with the help of streaming potential measurements. For the detection of amino (APTES) and carboxyl (TESPSA) groups, the anionic dye orange II and the cationic dye thionin acetate were used, respectively. Orange II quantification was based on a protocol by Bartels et al. [29]. APTES functionalized capillaries of 25 mm length were individually submerged in 1.75 mL of a 0.5 molar orange II solution in HCl of pH 3. They were incubated under constant shaking at 300 rpm and 21 °C for 24 h. Subsequently, the capillary pieces were washed three times in 10 mL HCl (pH 3) to remove any unbound orange II dye molecules. During the subsequent immersion of the capillaries in 2 mL of NaOH with pH 12 at 1000 rpm and RT for 15 min the dye molecules were released from the surface. In reference to a calibration curve of orange II dye in NaOH (pH 12), the molar amount was quantified photometrically by measuring the samples' absorbance at a wavelength of 483 nm (Multiskan GO, Thermo Scientific, Germany). Following the same principle, the carboxyl groups on TESPSA-functionalized membranes were determined as described by Ivanov et al. [30]. In our approach, the carboxylated capillaries were placed in a solution of thionin acetate in ethanol with a concentration of 24.42 mol/L (0.1 mg/mL) and incubated for 13 h at 21 °C. The capillaries were rinsed with ethanol before washing them in a 0.01 molar HCl solution in a 1:1 mixture of water and ethanol. The molar quantity of dye was estimated using thionin acetate's fluorescent behavior with excitation and emission wavelength at 595 nm and 618 nm, respectively (Chameleon plate reader, Hidex, Finland). Both photometric procedures were performed in triplicates.

The dependence of surface charge of oxidatively activated, aminated (APTES) and carboxylated (TESPSA) capillary membranes on the pH was characterized by determination of their zeta potential in streaming potential measurements. The experiments were conducted in

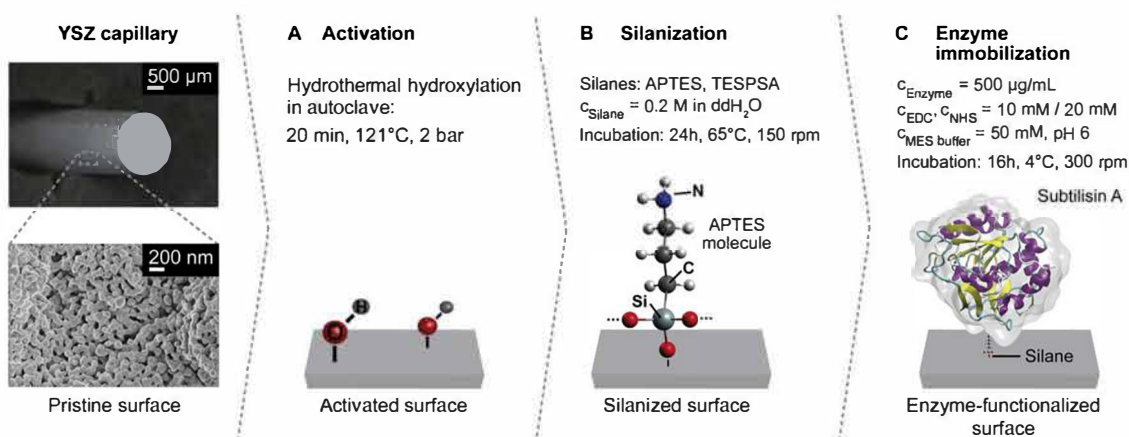


Fig. 1. Schematic of the surface modification process from pristine to enzyme-functionalized ceramic capillary membrane including (1) activation (hydroxylation), (2) silanization and (3) enzyme immobilization. APTES = (3-aminopropyl)triethoxysilane, EDC = 1-Ethyl-3-(3-dimethylaminopropyl)carbodiimid, MES = 2-(*N*-morpholino)-ethanesulfonic acid, NHS = *N*-Hydroxysuccinimide, TESPSA = 3(triethoxysilyl)propylsuccinicanhydride, YSZ = yttria stabilized zirconia.

agreement with Bartels et al. [29], using a custom designed electrokinetic analyzer and capillary measurement cell at the Institute of Electronic and Sensor Materials, Technische Universität Bergakademie Freiberg, Germany. The zeta potential of single 50 mm membranes was determined under crossflow filtration conditions, by measuring the streaming potential through the porous membrane walls between two Ag/AgCl-electrodes located at the feed and at the permeate side of the membrane. For the collection of single measurement points at a specific pH value, the capillary membrane was first rinsed with electrolyte of the respective pH for 20 s. Afterwards the trans-capillary membrane pressure was increased from 0 bar to a maximum pressure of 1 bar (100 kPa) in 20 s, and the streaming potential was concurrently measured, yielding the streaming potential coefficient (linear slope of the streaming potential – trans-membrane pressure straight) depending on the pH value. The zeta potential was then calculated from the streaming potential coefficient using the Helmholtz-Smoluchowski equation [31]. For each sample, the pH of the electrolyte was first increased to pH 9 and then lowered to pH 3 in pH steps of 0.25. The streaming potential measurements were conducted in triplicates. For comparison, single measurements were performed in the alternative overflow configuration.

2.3. Enzyme immobilization and quantification

The functionalized capillaries were used as supports for enzyme immobilization (Fig. 1C). Oxidatively activated, aminated (APTES) and carboxylated (TESPSA) capillaries were modified with subtilisin A in two different approaches. They were either immersed in a solution of enzyme in pure MES buffer or enzyme in MES buffer containing EDC and NHS (MES/EDC/NHS). Prior to enzyme immobilization, capillary membranes of 50 mm length were dead-end sealed using polysiloxane glue. Each capillary was incubated in 3.5 mL of subtilisin A solution with a concentration of 500 µg/mL in MES buffer (50 mmol/L, pH 6). To promote amide bond formation between functionalized membranes and protease, EDC and NHS were added to the enzyme solution in concentrations of 10 and 20 mM, respectively (MES/EDC/NHS). The capillaries were incubated for 16 h at 4 °C under shaking at 300 rpm. For each type of capillary and immobilization approach, three replicates were prepared.

By measuring the difference in enzyme concentration in the supernatant of the incubated capillaries before and after the experiment, the immobilized enzyme fraction was derived using a BCA photometric protein quantification kit [32]. The manufacturer's standard procedure for quantification of protein concentrations in microplates was carried out. The absorbance values of three supernatant samples per capillary were measured at a wavelength of 562 nm with a Multiskan GO photometer (Thermo Scientific, Germany). The protease concentrations in pure MES buffer or MES/EDC/NHS buffer were calculated based on individual reference curves.

The composition of the applied immobilization solutions before and after an incubation period of 16 h at 4 °C was investigated qualitatively using sodium dodecyl sulfate–polyacrylamide gel electrophoresis (SDS-PAGE) with subsequent silver staining. The industrial grade enzyme was compared to pure subtilisin A in both MES and MES/EDC/NHS buffer with and without addition of protease blocker to study possible effects of crosslinking and autolysis. The experimental set-up is detailed in the supplementary material (S4).

2.4. Enzyme leaching experiments

To evaluate the binding strength between immobilized enzymes and the capillary surfaces, enzyme leaching experiments were conducted. The experimental set-up (Fig. 2A) was based on Sewczyk et al., who described their configuration as plug flow reactor system (PFR) [21]. Single enzyme-modified capillaries (Fig. 2D) with dead end sealing were fixed inside custom designed stainless steel casings (Fig. 2B). At a

temperature of 25 °C, TRIS buffer (100 mmol/L, pH 7.8) was fed through three capillary reactors in parallel. Using a peristaltic pump (BVP, Ismatec, Germany), a constant crossflow rate of 134 µL/min from inside to outside of the membranes was achieved. Every six minutes, the flow was stopped to remove the individual permeates (800 µL) and store them at 4 °C for later testing. After approximately two hours, 20 permeate samples with a total volume of 16 mL were collected and tested for their enzyme concentration with a photometric Bradford protein quantification kit [33]. For the quantification of protein concentrations in microplates the manufacturer's standard Micro-Bradford procedure was followed. Of each permeate sample, three replicates were investigated concerning their absorbance at a wavelength of 595 nm (Multiskan GO, Thermo Scientific, Germany). The enzyme concentrations were determined based on reference curves. The permeate samples were differentiated by the type of capillary functionalization into unfunctionalized (reference), APTES (aminated) and TESPSA (carboxylated) linkers and by buffer composition of the immobilization solution into pure MES and MES/EDC/NHS buffer.

2.5. Determination of specific enzyme activity

The specific enzyme activity of immobilized subtilisin A was measured photometrically by monitoring the enzymatic degradation of the synthetic substrate Boc-Ala-ONp to 4-nitrophenol [34]. Based on Sewczyk et al., an 80 mM stock solution of Boc-Ala-ONp in a 4:1 mixture of acetonitrile and TRIS buffer (pH 7.8) was prepared [21]. To evaluate the activity of enzymes, which were immobilized on capillaries with different types of functionalization (unfunctionalized, APTES, TESPSA) using MES/EDC/NHS buffer, this stock solution was further diluted with TRIS buffer in a ratio of 1:100. Per sample, 3.03 mL of the assay were pipetted into single cavities of a 6-well microplate. Capillary samples were prepared by cutting 5 mm pieces from an enzyme-modified capillary, which had been washed with 5 mL of buffer as described above. One sample was added to the assay solutions per well. Immediately after, the measurement of the samples' absorbance at a wavelength of 405 nm and a temperature of 30 °C was started (Chameleon, Hidex, Finland). Under intermittent shaking, the samples were observed over a period of 10 min. The molar amount of product, i.e. 4-nitrophenol, was calculated based on reference curves using 4-nitrophenol in the corresponding solvent. From this, the specific enzyme activity was determined as the coefficient of linear product increase with time (µmol/min) divided by the mass of immobilized enzyme (mg). Additional experiments regarding the activity of free enzyme as well as the influence of pH and temperature on the specific activity of both immobilized and free subtilisin A are detailed in the supplementary material (S5). All activity experiments were conducted in triplicates. For each buffer pH, individual reference curves were prepared.

2.6. Continuous proteolysis and peptide analysis

The digestion of casein as the model protein was performed both online using proteolytic capillaries as well as under static conditions with free enzyme at a temperature of 25 °C. For the hydrolysis under flow by capillary reactors, membranes (unfunctionalized, APTES, TESPSA) which had been modified by subtilisin A in MES/EDC/NHS buffer were investigated. Prior to casein hydrolysis, the membranes were flushed with 5 mL of TRIS buffer as described above. The proteolysis was conducted using the same set up as for enzyme leaching experiments (Fig. 2), but with casein solution ($c = 0.5$ g/L in 100 mM TRIS buffer, pH 7.8) as feed and a reduced flow rate of 44 µL/min. The first 140 µL of casein hydrolysate were discarded to avoid dilution effects from the TRIS buffer solution. Afterwards, per capillary reactor, 1 mL of permeate was collected in single containers holding 0.12 mg of Pefabloc® SC protease inhibitor. The proteolysis of casein with free enzyme was conducted using a solution of subtilisin A with a concentration of 1 mg/mL in TRIS buffer. 0.5 mL of protease solution were

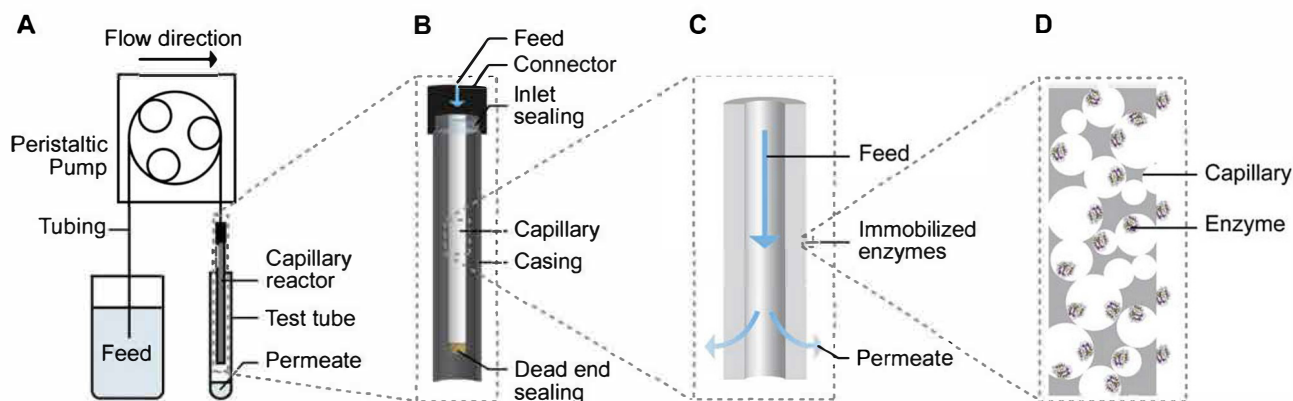


Fig. 2. (A) Schematic of the experimental set-up used for enzyme wash-out quantification and protein digestion experiments. (B) Detailed sketch of the inside of the enzymatic reactor with capillary in dead-end mode. (C) Cross-sectional schematic of the ceramic capillary membrane with indication of crossflow direction. (D) Representation immobilized enzyme molecules on the capillary surface.

added to 2 mL of casein feed. The reaction was stopped after 30 min by the addition of 0.6 mg of Pefabloc® SC protease inhibitor. For all sample types, three replicates were prepared and stored at 4 °C until further analysis.

The peptide composition of casein hydrolysates was investigated at the Institute for Technical Chemistry, Leibniz University Hannover, using HPLC according to Sewczyk et al. [21]. A reversed phase column (Aeris™ 3.6 µm PEPTIDE XB-C18 100 Å, LC Column 250 × 4.6 mm, Ea, Phenomenex, USA) with guard cartridge (SecurityGuard™ Standard, C18, Phenomenex, USA) was used for separation. Details on the experimental procedure can be reviewed in the supplementary material (S6). All samples were analyzed in duplicates and compared against the analytical peptide standard.

The degree of hydrolysis of capillary digests was estimated semi-quantitatively by peak area integration. After linear baseline correction of each HPLC chromatogram, the overall peak area of the casein feed was determined between $x = 63.4$ and 70.0 min. The peak area of the capillary digests was compared to the casein feed solution. For each type of proteolytic capillary, three chromatograms were investigated.

2.7. Modeling of the enzyme's structure and electrostatic surface potential

Structural data for modeling of subtilisin A was supplied by entry 1SBC [35] of the Research Collaboratory for Structural Bioinformatics Protein Data Bank (RCSB PDB, <https://www.rcsb.org/>). The PDB file was converted into PQR format using the PDB2PQR web service (http://nbc-222.ucsd.edu/pdb2pqr_2.1.1/) [36] with the PARSE parameter set (parameters for solvation energy) [37] and the PROPKA software for prediction of protonation states [38] at pH 6. The PQR file contained additional force field parameters such as atomic charge and radii and served as input data for the Adaptive Poisson-Boltzmann Solver (APBS) [39]. The APBS (http://nbc-222.ucsd.edu/pdb2pqr_2.1.1/) was used to calculate the electrostatic surface potential distribution of subtilisin A at 25 °C in water. For the visualization of the enzymatic structure and its electrostatic surface potential the software Visual Molecular Dynamics (VMD) [40] was used.

3. Results and discussion

3.1. Effect of surface functionalization

To evaluate the influence of surface functionalization on the properties of immobilized protease, porous ceramic capillaries were chemically modified using the aminosilane APTES and the carboxysilane TESPSA to yield aminated and carboxylated surface, respectively. Prior to silanization, the unfunctionalized capillaries were characterized by a unimodal pore size distribution with an open porosity of

$53.26 \pm 1.32\%$, a pore window size mode of 82.00 ± 0.51 nm and a specific surface area of 6.70 ± 0.72 m²/g. The macroscopic geometry and microstructure of these capillaries is depicted in Fig. 1A. Their characteristic biaxial bending strength and Weibull modulus amounted to 42.08 MPa and 17.16, respectively. APTES and TESPSA functionalization resulted in insignificant changes in the observed microstructure, porous properties, surface area and strength, i.e. silanization did not affect both microstructure and mechanical properties of the ceramic support materials. Therefore, influences by these factors on interactions between the enzyme and the porous structure of capillaries can be excluded in the following. Detailed data including SEM images (Figure S3.1), representative pore size distributions (Figure S3.2) and Weibull distributions (Figure S3.3) of all capillary types can be found in the supplementary material (S3).

The success of surface functionalization via silanization was however confirmed by photometric assays and streaming potential analysis (Fig. 3). The coverage of the capillaries pore structure with functional groups was determined to be in the same order of magnitude for both APTES- and TESPSA-functionalized surfaces (Fig. 3A) with twice the amount of accessible amino groups (0.43 ± 0.00) compared to carboxyl groups per nm² (0.22 ± 0.02). The maximum theoretical amount of functional groups per nm² in regular monolayer configuration [41] can be roughly estimated to 1.12 amino groups and 2.84 carboxyl groups per nm². During functionalization, water molecules are needed to hydrolyze the APTES and TESPSA molecules to form more reactive silanols and ethanol [15]. Thus, the water content in the solvent medium is used to tailor the degree of silane hydrolysis [15]. Since both APTES and TESPSA molecules carry three ethoxy groups, this consequently defines the degree of crosslinking between silane molecules and between silane molecules and support [15]. Considering the silanization protocol used, which was carried out in water for 24 h, a silane multilayer coverage of the surface is thus more likely than monolayer formation [15]. But since the assay-derived number of functionalities only describes the accessible terminal surface groups rather than the total amount, the same measured maximum amount of functional groups can be assumed for mono- and multilayer configuration. Compared with the determined amount of accessible functional groups, only approximately 38% and 8% of the maximum densities were reached in case of APTES and TESPSA, respectively.

The results from the streaming potential measurements under crossflow filtration conditions show that the surface charge of the capillaries was altered as an effect of silanization with APTES and TESPSA (Fig. 3B), as has been described previously [20,29,42]. The isoelectric point (IEP) of the reference capillaries was determined to be at pH 7.7 ± 0.5 , while both types of silanized capillaries did not reach a neutral surface charge within the investigated range from pH 3 to 9. The determined IEP of the reference is in reasonable agreement with

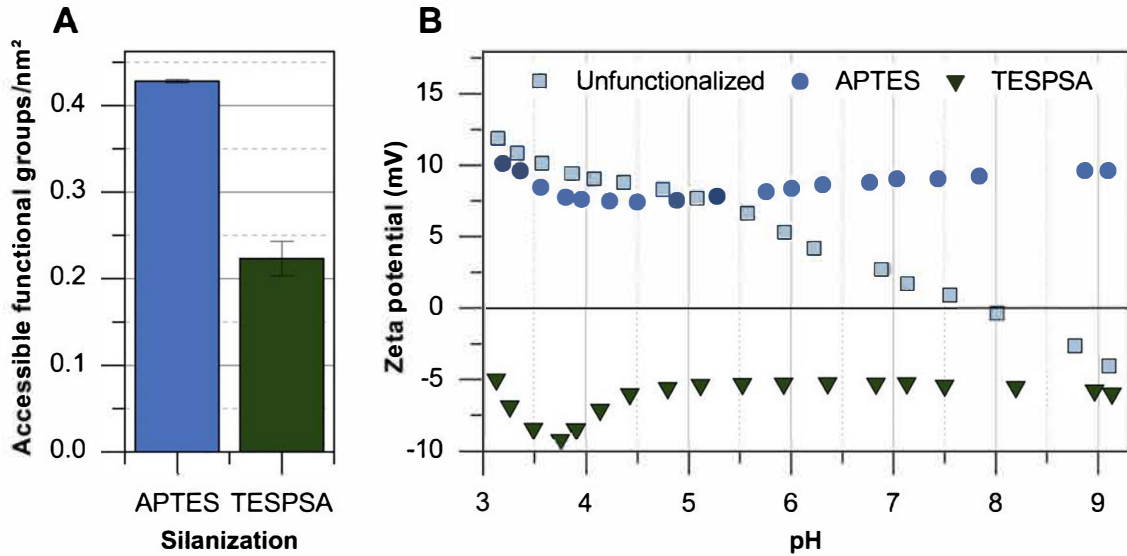


Fig. 3. (A) Amount of accessible functional groups per nm² of capillary surface after silanization with different silanes. Error bars are indicating the standard deviations between 3 replicates. (B) Representative streaming potential curves of unfunctionalized (reference) and silanized capillaries under crossflow filtration conditions.

reported values for pure, water-dispersed YSZ powder (TZ-3Y-E) of 9.0 [43], while studies on a very similar powder from the same manufacturer (TZ-3Y) presented IEPs between pH 6 and 8 [44–46]. In a range from approximately pH 5 to 9, aminated capillaries showed a more positive zeta potential than the unfunctionalized reference, while carboxylated membranes were characterized by a more negative surface charge throughout the whole investigated pH range. Single streaming potential measurements of all capillary types under overflow filtration conditions exhibit the same trend (see supplementary material, Figure S6.1).

3.2. Surface coverage and binding strength of immobilized enzymes

Using both MES buffer solutions with and without EDC and NHS, subtilisin A was successfully immobilized on unfunctionalized, APTES- and TESPSA-functionalized capillaries (Fig. 4A). Using the EDC/NHS

reaction mechanism, amide bond formation between either activated carboxylates on the enzyme's surface (side chains of aspartic and glutamic acid residues, C-terminus) and amino groups on the immobilization support (APTES) or between activated carboxylates on the immobilization support (TESPSA) and accessible amino groups on the enzyme's surface (side chains of lysine residues, N-terminus) was facilitated. Since the same amount of lysine side chains (8 amino groups) compared to aspartic and glutamic acid side chains (8 carboxyl groups in sum) are present on the enzyme's surface [47], both binding of the enzyme to carboxylated and aminated surfaces should be possible. However, if these functional groups were not or not sufficiently available on either immobilization support or enzyme, all or fractions of the enzymes might have non-covalently attached to the surface, e.g. by hydrophobic, Van der Waals's or ionic interactions. Independent of the immobilization approach (MES/EDC/NHS or MES), the highest enzyme density was achieved on carboxylated capillaries, with 0.016 ± 0.002

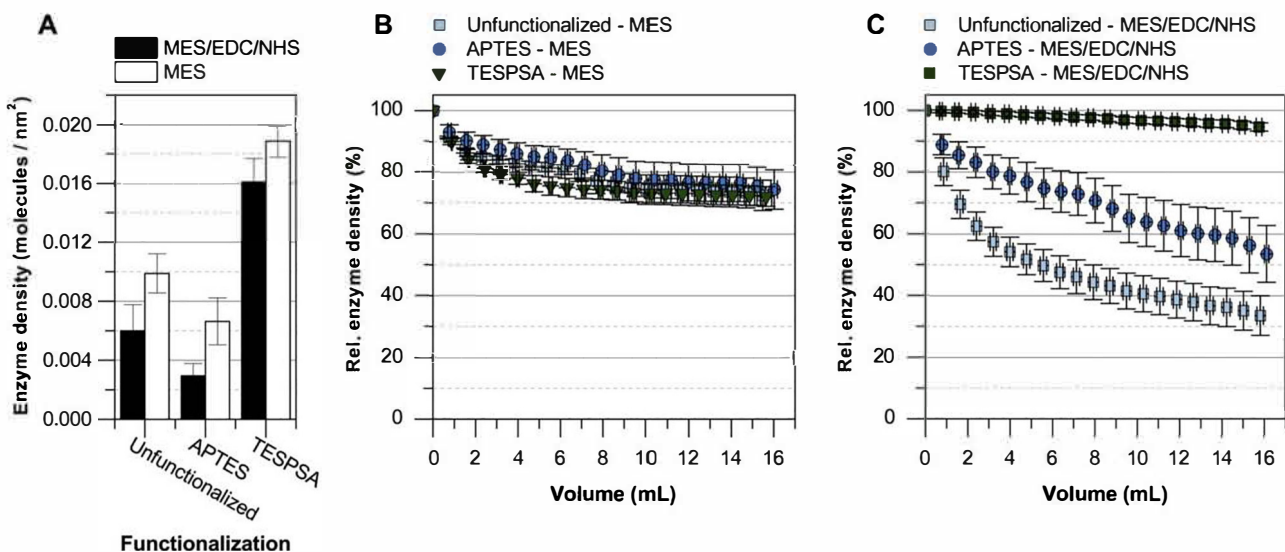


Fig. 4. (A) Initial enzyme density (subtilisin A) (molecules/nm²) on ceramic capillary membranes differentiated by surface functionalization into unfunctionalized (reference), aminated (APTES) and carboxylated (TESPSA) as well as by the immobilization approach (MES, MES/EDC/NHS). (B, C) Enzyme leaching from capillaries during washing with a defined volume of buffer solution: (B) Capillaries modified by enzyme in pure MES immobilization solution, (C) Capillaries modified by enzyme in MES/EDC/NHS immobilization solution. Error bars are indicating the standard deviations between 3 replicates.

molecules/nm² on MES/EDC/NHS and 0.019 ± 0.001 molecules/nm² on MES treated capillaries. A coverage of 0.006 ± 0.002 molecules/nm² and 0.010 ± 0.001 molecules/nm² was achieved on the unfunctionalized reference capillaries in the MES/EDC/NHS and MES immobilization approach, respectively. The smallest enzyme densities were detected on APTES-functionalized capillaries, which featured 0.003 ± 0.000 molecules/nm² after MES/EDC/NHS treatment and 0.007 ± 0.002 molecules/nm² after MES treatment. Thus, the mean amount of enzyme molecules per nm² of capillary were in the same order of magnitude for all three types of samples, but they did not seem to be directly correlated to the amount of accessible functional groups (Fig. 3A). Although most functional groups were present on aminated surfaces, the highest amounts of enzyme molecules per area were immobilized on carboxylated surfaces. However, electrostatic interactions are known to be an important parameter in enzyme immobilization [12,48,49]. In our case, the coverage of the surface with enzymes appeared to be related to the zeta potential of both capillary and enzyme at pH 6, which was applied during immobilization. At this pH, APTES-functionalized, aminated capillaries were characterized by the highest zeta potential of 8.95 ± 0.97 mV (pH 6.02 ± 0.07), while unfunctionalized and TESPSA-functionalized, carboxylated capillaries featured zeta potentials of 5.16 ± 0.40 mV (pH 6.05 ± 0.10) and -5.45 ± 0.54 mV (pH 5.97 ± 0.08), respectively. Since the IEP of subtilisin A is 9.4 [50], the enzyme is charged positively at a pH of 6. Therefore, during immobilization, based on net charge subtilisin A would be most strongly attracted towards the negatively charged carboxylated surface, less attracted to the unfunctionalized reference and least attracted to the aminated surface. The overall electrostatic potential of both support and enzyme surface is defined by the sum of charged functional groups. Although this concept does not factor in localized deviations and distributions in charge on the enzyme surface, it indicates the strength of ion cloud interactions leading to adsorption and eventually the formation of a large number of ionic bonds between enzyme and support based on the number of available oppositely charged functional groups. If a regular two-dimensional monolayer configuration [51] of the immobilized enzymes is assumed and they are treated like hard spherical particles without any electrostatic interactions, the theoretical maximum protein coverage can be calculated as 0.05 enzymes per nm². Thus, by immobilization of subtilisin A on a carboxylated surface using pure MES, a coverage of 34% was reached, while the use of MES/EDC/NHS on an APTES-functionalized membrane resulted in only 5% coverage of the maximum enzyme density.

In general, enzyme immobilization in pure MES buffer resulted in slightly higher initial enzyme densities on the capillary surface compared to immobilization in MES/EDC/NHS (Fig. 4A). SDS-PAGE analysis of the applied immobilization solutions suggests that the addition of EDC and NHS actually led to the formation of reactive ester intermediates at the surface of the enzymes [15]. As a result of EDC and NHS addition, the apparent molecular weight of subtilisin (band close to a molecular weight of 31 kDa, see supplementary material Figure S4.1) appeared to be increased, i.e. compared to pure buffer immobilization solutions, the protein bands were shifted towards larger molecular weights. The formation of reactive complexes with the carboxylic groups on the enzyme's surface could further have an influence on the surface charge of the enzyme, on resulting electrostatic interactions between enzyme and support and thereby on the enzyme loading during immobilization using EDC and NHS. Analogously, EDC and NHS might also change the surface potential of carboxylated supports (TESPSA).

The immobilization approach (MES/EDC/NHS or MES) influenced the enzymes' resistance to leaching under flow conditions (Figure 4b/c). While the silane coating can be considered as stable under flow [29], not all of the immobilized enzyme will necessarily be stably bound to the surface. During leaching experiments, weakly bound molecules, such as non-covalently attached enzymes (hydrophobic, Van der Waals's or ionic interactions), were washed from the membrane by the

buffer solution. Thus, leaching experiments were used to evaluate the extent of covalent enzyme binding compared to an unfunctionalized reference. Since there are neither amino nor carboxyl groups present on the unfunctionalized capillary, no amide bonds will be formed between enzyme and unfunctionalized support and the enzymes should be removed quickly. Concerning enzyme wash-out, all three types of capillaries, which were incubated in pure MES immobilization solution, exhibited a very similar behavior (Fig. 4B): After flushing with 16 mL of buffer, 72–74 % of the initial enzyme remained on the surface. TESPSA- and APTES-treated membranes behaved like the unfunctionalized reference, which indicates that without the use of EDC and NHS indeed no covalent bonds between protease and any type of support were formed. Capillaries, which were immobilized using EDC and NHS, exhibited distinct differences in enzyme leaching with respect to functionalization type (Fig. 4C). After flushing, only 34% of the initially adsorbed subtilisin A eventually remained on the unfunctionalized membrane surface. Compared to this reference, the addition of EDC and NHS resulted in a higher binding strength to TESPSA functionalized surfaces with 95% of the enzyme remaining on the surface. Thus, it can be assumed that amide bonds between carboxyl groups on the capillary surface and primary amino groups (side chains from lysine residues, N-terminus) on the enzyme formed during immobilization. Covalently bound enzymes would have a higher resistance to wash-out and therefore only 5% of presumably non-covalently, more loosely attached enzymes is removed. The use of EDC and NHS was less effective with respect to APTES functionalized capillaries. In this case, 54% of the initial amount of attached enzyme remained on the surface. This indicates an increased enzyme stability compared to unfunctionalized capillaries and thus some degree of covalent binding between carboxyl groups on the enzyme's surface (side chains of aspartic and glutamic acid residues, C-terminus) and amino groups from the support. Nonetheless, the enzyme leaching is much greater as observed in TESPSA functionalized capillaries and suggests that most of the enzyme molecules are actually non-covalently bound. Accordingly, covalent binding seemed to be more successful between the carboxylated surface and positively charged amino groups of the enzyme, than between aminated surface and the enzyme's carboxyl groups. The resistance of the enzymes against wash-out did not correlate with the amount of different accessible functional groups on the support surface, but it appeared to be related to the charge of both surface and the enzyme. Up to its IEP at pH 9.4 subtilisin A is characterized by predominantly positively charged amino acid residues on the enzyme's surface [15,50,52].

It must be noted that the wash-out is expressed relative to the initial enzyme density (Figure 4B/C), which was smaller in case of incubation in MES/EDC/NHS compared to incubation in pure MES buffer (Fig. 4A). However, the absolute amount of removed enzyme was in the same range. Thus, the observed leaching rates are systematically larger for enzyme immobilized via MES/EDC/NHS as compared to enzyme immobilized in pure MES.

3.3. Immobilized enzyme activity

Although the TESPSA functionalization was effective in increasing the amount of immobilized enzyme molecules and their stability under flow conditions, it appears to have an adverse impact on the specific activity of immobilized subtilisin A (Fig. 5). After immobilization, subtilisin on unfunctionalized and APTES-functionalized capillaries is characterized by a similar specific activity of $0.99 \mu\text{mol}/\text{min}/\text{mg}$ of immobilized enzyme, while on TESPSA capillaries the enzyme exhibited a specific activity of only $0.15 \mu\text{mol}/\text{min}/\text{mg}$. In case of the reference and aminated immobilisates, this represents approximately 8% of the specific activity of the free in enzyme in MES/EDC/NHS ($11.46 \mu\text{mol}/\text{min}/\text{mg}$), but only 1% in case of enzymes immobilized on carboxylated supports. On the one hand, the similarity in specific activity between reference and APTES-functionalized capillary could be an additional indication that covalent binding to APTES amino groups

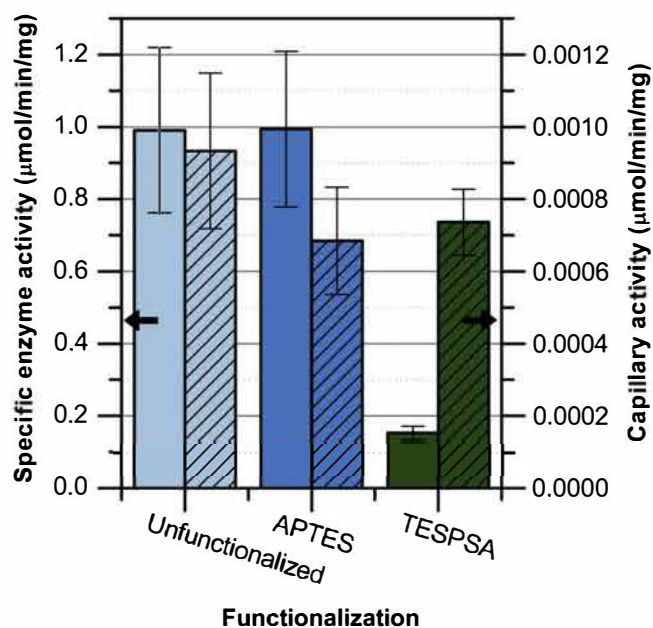


Fig. 5. Specific enzyme activity (non-patterned columns) and capillary activity (patterned columns) given as activity per mass ($\mu\text{mol}/\text{min}/\text{mg}$) of immobilized enzyme and per mass of capillary, respectively. Enzymes were immobilized on functionalized membrane surfaces using the MES/EDC/NHS approach. Error bars are indicating the standard deviations between 3 replicates.

was not successful. On the other hand, it is possible that the covalent binding of subtilisin A to APTES linker molecules does not alter specific activity as compared to non-covalent adsorption by e.g. preserving the enzyme's conformation during immobilization.

Upon pH variation, an increase in enzyme activity is observed for both immobilized and free enzyme when approaching the enzyme's pH optimum between 8 and 11 [50,53] (Figure S.5.1 A). A small temperature variation $30 \pm 5^\circ\text{C}$ did not indicate a trend regarding specific enzyme activity (Figure S.5.1B). Independent of pH and temperature conditions, the overall proportionality between specific activity of immobilized enzyme on different support materials and free enzyme was maintained, which again suggests that enzyme performance is mostly defined by the nature of enzyme binding to varying membrane types (unfunctionalized, APTES and TESPSA-functionalized).

Although a decrease of specific enzyme activity due to enzyme denaturation during immobilization is a common phenomenon [10,12], subtilisin A is characterized as a 'hard' enzyme, that consequently does not unfold or denature easily when in contact with a surface [54]. Nevertheless, in our system, the strongest electrostatic interactions are expected between subtilisin A and the carboxylated surface, so any ionic-bond induced conformational changes of the enzyme should be most pronounced in TESPSA-functionalized capillaries. A loss of enzyme motility in case of TESPSA is also possible, since the bonds between ceramic capillary and enzyme appear to be stronger compared to APTES-functionalized and unfunctionalized capillaries (Fig. 4C). Additionally, enzyme activity could be reduced by non-optimum enzyme orientation. One disadvantage of uncontrolled (covalent) immobilization, is the fact, that the enzymes' catalytic site could be blocked in the process [10]. For subtilisin BPN', which is structurally very similar to subtilisin A [50], Huang et al. detected improved enzyme activity, when the active site was specifically oriented away from the support [55]. In subtilisin A, the active center is represented by a catalytic triad of aspartic acid, histidine and serine amino acid residues (Fig. 6A/B) [56,57]. The surface potential of the enzyme at pH 6, 25°C in water is illustrated in Figure 6C/D. The active site is charged positively and the side opposite to the catalytic triad is characterized by an overall more neutral surface. It is therefore possible that during initial adsorption of

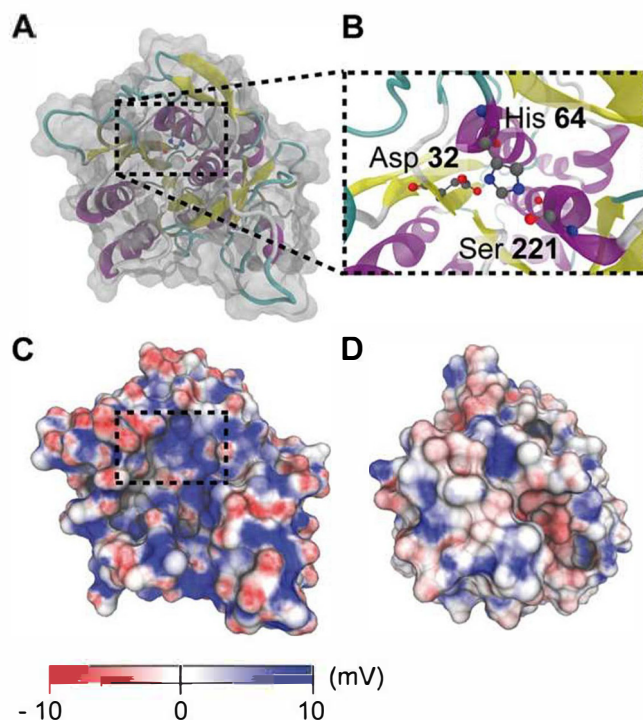


Fig. 6. Location of the enzymatic active center and electrostatic surface potential of subtilisin A. (A) Protease secondary structure and solvent accessible surface. The location of the active site is indicated by dashed lines. (B) Close up of the catalytic triad consisting of amino acid residues of aspartic acid 32, histidine 64 and serine 221. (C, D) Distribution of the electrostatic potential on the water accessible protease surface at 25°C and pH 6. The negative and positive charge (mV) is labelled in red and blue, respectively. In (C), the position of the catalytic center is indicated by dashed lines. (D) represents the enzyme surface opposite to the active site, i.e. opposite to (C) (For interpretation of the references to colour in this figure legend, the reader is referred to the web version of this article.).

subtilisin A on a negatively charged TESPSA membrane, the enzymes orient with their catalytic centers directed towards the support material. This would block the active site and explain the reduced specific enzyme activity in the case of TESPSA. The addition of competitive inhibitors during immobilization [10] could potentially be used to avoid binding of TESPSA to the enzyme's active center. Considering the low specific activity of TESPSA immobilisates regarding both the small synthetic substrate Boc-Ala-ONp and the large substrate casein, it is likely that immobilization on carboxylates to some degree resulted in the inactivation of enzyme molecules e.g. by conformational changes, which has been previously described by Tardioli et al. [58].

Considering the activity of proteolytic capillaries as a whole, not only the specific activity of the immobilized enzymes plays an important role, but also the amount of immobilized enzyme molecules per mass of capillary. Although immobilized enzymes on e.g. TESPSA-functionalized surfaces displayed by far the smallest specific enzyme activity (Fig. 5, non-patterned columns), they featured the highest enzyme density (Fig. 4A). If these two factors are taken into account, the 'capillary activity' of all three types of capillaries, which should be understood as the activity ($\mu\text{mol}/\text{min}$) per mass of capillary (mg), is in a similar range (Fig. 5, patterned columns): APTES- and TESPSA-functionalized membranes exhibited a capillary activity of 6.8 ± 1.5 and $7.4 \pm 0.9 \cdot 10^{-4} \mu\text{mol}/\text{min}/\text{mg}$, respectively, while unfunctionalized capillaries had a capillary activity of $9.3 \pm 2.2 \cdot 10^{-4} \mu\text{mol}/\text{min}/\text{mg}$. Even though the highest capillary activity was thus related to unfunctionalized capillaries, covalent immobilization on functionalized supports might still be of advantage in specific applications. Enzyme immobilization has shown to potentially increase the resistance of

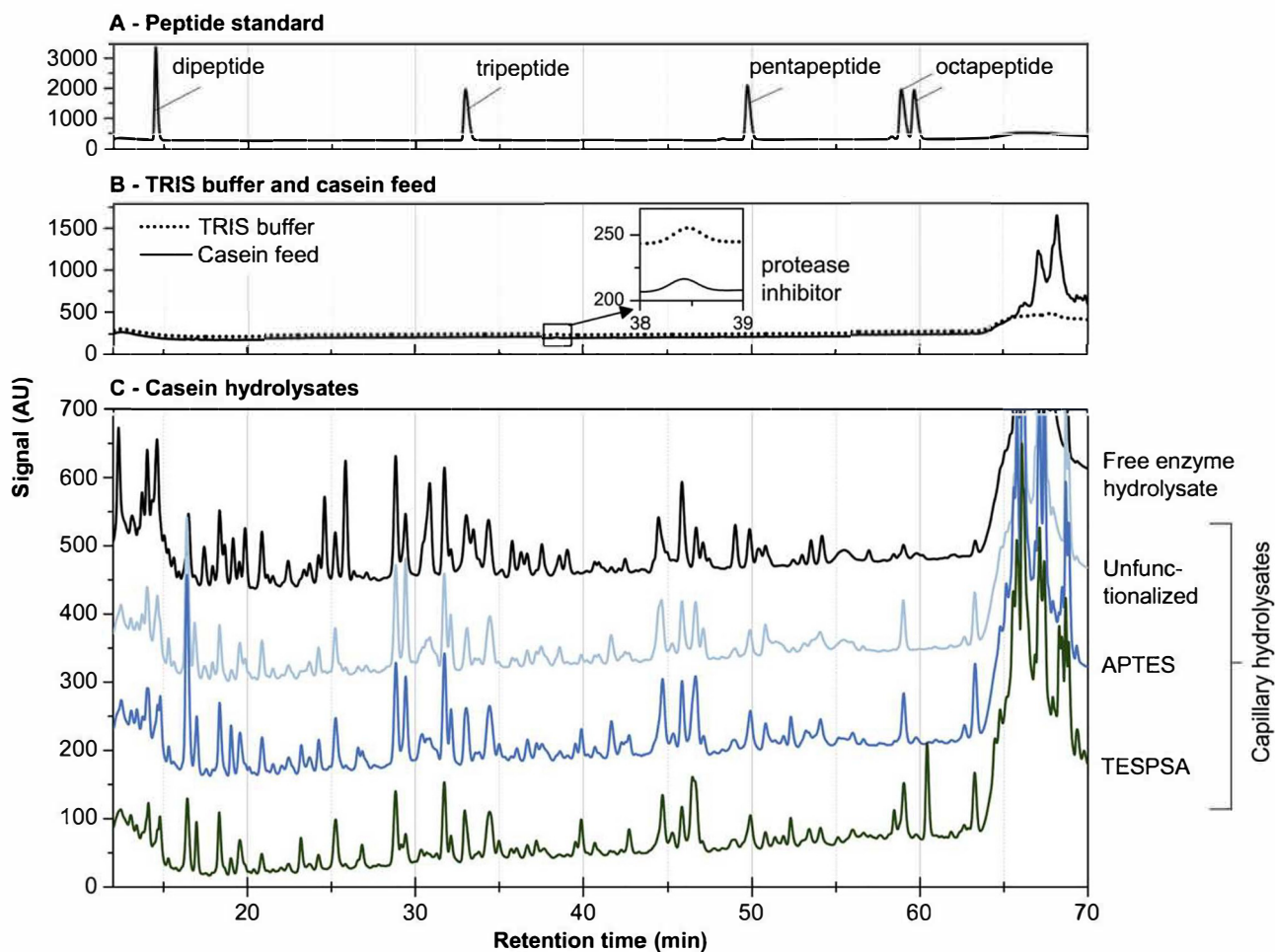


Fig. 7. Peptide spectra as determined by HPLC analysis: (A) Peak positions of bipeptides, tripeptides, pentapeptides and octapeptides in peptide standard, (B) Chromatograms of TRIS buffer and casein feed solution with protease inhibitor, (C) Peptide spectra of casein feed solution hydrolyzed with free (native) enzyme and under continuous flow using proteolytic, functionalized (unfunctionalized, APTES, TESPSA) capillaries.

enzymes against harsh pH and temperature conditions under repeated use [10]. Long-term experiments could indicate, whether the use of either APTES- or TESPSA-functionalized protease supports would prove beneficial e.g. under extreme conditions. When immobilizing alcalase on monoaminoethyl-*N*-aminoethyl-agarose beads, Ait Braham recently showed that the resulting enzyme activity with respect to casein was influenced by the pH during immobilization [59]. Thus, the specific activity of proteolytic capillaries might be improved by changing the pH conditions of the immobilization process.

3.4. Continuous peptide production of enzyme-modified capillaries

HPLC analysis of the protein hydrolysates showed that all investigated types of proteolytic capillaries (unfunctionalized, APTES- or TESPSA-functionalized) could be successfully used to produce peptides from casein under flow conditions (Fig. 7). However, specific differences between the derived peptide spectra were found (Fig. 7C). Prior to hydrolysis, HPLC showed clearly that the casein feed consisted of a mixture of different large polypeptides, i.e. casein types (Fig. 7B). During digestion, these casein molecules are hydrolyzed and smaller peptides are formed (Fig. 7C). Although the reaction conditions during digestion of the feed protein in a static set up using free enzyme and under flow with proteolytic capillaries were very different, similar peptide fractions were produced with both approaches (Fig. 7C). This indicates that the specificity of the enzymes was not strongly altered upon immobilization. The main difference between all four hydrolysates – free enzyme and capillary derived – is the varying amount of

specific peptide fractions in the samples. The TESPSA membrane hydrolysates contain significant amounts of molecules in the octapeptide range, while some of these compounds are barely present in the hydrolysates of unfunctionalized and APTES capillary as well as in free enzyme digests (Fig. 7C). In contrast to this, the casein hydrolysates of unfunctionalized and APTES-functionalized membranes presented more dipeptides and tripeptides than TESPSA capillary digests. This indicates a higher degree of casein hydrolysis compared to TESPSA membranes, which correlates with the decreased specific enzyme activity of subtilisin on TESPSA and might also indicate small changes in enzyme specificity due to covalent binding to carboxylated supports (Fig. 5, non-patterned columns). Semiquantitatively, the degree of hydrolysis of the three membrane hydrolysates was estimated by peak area integration to $55 \pm 1\%$ for unfunctionalized capillaries, $57 \pm 2\%$ for APTES-treated membranes and $52 \pm 2\%$ for TESPSA-functionalized samples. This again suggest a higher proteolytic activity of unfunctionalized and APTES capillaries versus TESPSA membranes, although the differences in degree of hydrolysis are small compared to the variations in specific enzyme activity (Fig. 5, non-patterned columns). However, they are in reasonable agreement with the total capillary activity, which relates specific enzyme activity with the density of immobilized enzymes and was very similar for all three capillary types (Fig. 5, patterned columns). Limitations in the transferability of capillary activity from photometric assay analysis to the actual performance of the proteolytic capillaries in casein hydrolysis can still be expected: On the one hand due to the size difference between the synthetic substrate Boc-Ala-ONp and the protein casein, on the other hand, due to the different reaction

conditions (batch vs. flow). With a variation of flow rates, it should be possible to vary the residence time of the substrate inside the proteolytic capillaries. This way it should be possible to produce very similar peptide spectra from enzyme-modified membranes with different capillary activity [21].

4. Conclusions

We were able to obtain proteolytic membranes from ceramic capillaries with varying surface functionalizations. The applied laboratory scale set-up was successfully used to evaluate the effect of different surface treatments on the immobilization of subtilisin A and the production of peptides under flow conditions. It was shown that silane molecules with different functional groups can be used to efficiently alter the surface properties of YSZ membranes and allow for the immobilization of enzymes on the surface. The type of silane was crucial for the initial adsorptive binding of enzymes, the formation of stable covalent bonds between enzymes and linker molecules, the specific enzyme activity and the resulting composition of the protein hydrolysate. These differences were largely related to the surface charge in relation to the amino acid composition of the enzyme. In consequence, surface interactions of proteases should be carefully considered when immobilized enzymes are envisioned for the production of peptides. In the investigated case, high binding strength of the enzyme to the support's surface comes at the cost of lowered specific activity. We demonstrated that our approach can be successfully used to immobilize proteases for peptide production and to tailor the immobilized enzyme's performance in a membrane reactor set-up via different surface functionalizations.

Conflict of interest

The authors have no conflict of interest to declare.

Acknowledgements

The authors are grateful for funding by the DFG through grant KR 3802/5-1 and to Novozymes A/S, Denmark, for providing the Alcalase® 2.5.

Appendix A. Supplementary data

Supplementary material related to this article can be found, in the online version, at doi:<https://doi.org/10.1016/j.bej.2019.04.005>.

References

- J.L. Lau, M.K. Dunn, Development trends for peptide therapeutics: status in 2016, 11th Annual Peptide Therapeutics Symposium La Jolla (2016).
- D.D. Kitts, K. Weiler, Bioactive proteins and peptides from food sources. Applications of bioprocesses used in isolation and recovery, *Curr. Pharm. Des.* 9 (2003) 1309–1323.
- H. Korhonen, A. Pihlanto, Bioactive peptides: production and functionality, *Int. Dairy J.* 16 (2006) 945–960.
- D. Agyei, M.K. Danquah, Industrial-scale manufacturing of pharmaceutical-grade bioactive peptides, *Biotechnol. Adv.* 29 (2011) 272–277.
- S.-K. Kim, I. Wijesekara, Development and biological activities of marine-derived bioactive peptides: a review, *J. Funct. Foods* 2 (2010) 1–9.
- O.L. Tavano, A. Berenguer-Murcia, F. Secundo, R. Fernandez-Lafuente, Biotechnological applications of proteases in food technology, *Compr. Rev. Food Sci. Food Saf.* 17 (2018) 412–436.
- R.A. Sheldon, Enzyme immobilization: the quest for optimum performance, *Adv. Synth. Catal.* 349 (2007) 1289–1307.
- R.A. Sheldon, S. van Pelt, Enzyme immobilisation in biocatalysis: why, what and how, *Chem. Soc. Rev.* 42 (2013) 6223–6235.
- C. Garcia-Galan, Á. Berenguer-Murcia, R. Fernandez-Lafuente, R.C. Rodrigues, Potential of different enzyme immobilization strategies to improve enzyme performance, *Adv. Synth. Catal.* 353 (2011) 2885–2904.
- S. Chakraborty, H. Rusli, A. Nath, J. Sikder, C. Bhattacharjee, S. Curcio, E. Drioli, Immobilized biocatalytic process development and potential application in membrane separation: a review, *Crit. Rev. Biotechnol.* 36 (2016) 43–58.
- C. Mateo, J.M. Palomo, G. Fernandez-Lorente, J.M. Guisan, R. Fernandez-Lafuente, Improvement of enzyme activity, stability and selectivity via immobilization techniques, *Enzyme Microb. Technol.* 40 (2007) 1451–1463.
- S.B. Sigurdardóttir, J. Lehmann, S. Ovtar, J.C. Grivel, M.D. Negra, A. Kaiser, M. Pinelo, Enzyme immobilization on inorganic surfaces for membrane reactor applications: mass transfer challenges, enzyme leakage and reuse of materials, *Adv. Synth. Catal.* (2018).
- R.C. Rodrigues, C. Ortiz, Á. Berenguer-Murcia, R. Torres, R. Fernández-Lafuente, Modifying enzyme activity and selectivity by immobilization, *Chem. Soc. Rev.* 42 (2013) 6290–6307.
- S. Datta, L.R. Christena, Y.R.S. Rajaram, Enzyme immobilization: an overview on techniques and support materials, *3 Biotech* 3 (2013) 1–9.
- G.T. Hermanson, *Bioconjugate Techniques*, Elsevier, Oxford, 2013.
- J. Zdzarta, A.S. Meyer, T. Jesionowski, M. Pinelo, A general overview of support materials for enzyme immobilization: characteristics, properties, practical utility, *Catalysts* 8 (2018) 92.
- H. Salmang, H. Scholze, R. Telle, *Keramik*, Springer, 2007.
- G.M. Rios, M.P. Belleville, D. Paolucci, J. Sanchez, Progress in enzymatic membrane reactors – a review, *J. Membr. Sci.* 242 (2004) 189–196.
- R. Brady, B. Wootton, M.L. Gee, A.J. O'Connor, Hierarchical mesoporous silica materials for separation of functional food ingredients — a review, *Innov. Food Sci. Emerg. Technol.* 9 (2008) 243–248.
- S. Kroll, C. Brandes, J. Wehling, L. Treccani, G. Grathwohl, K. Rezwan, Highly efficient enzyme-functionalized porous zirconia microtubes for Bacteria filtration, *Environ. Sci. Technol.* 46 (2012) 8739–8747.
- T. Sewczyk, M. Hoog Antink, M. Maas, S. Kroll, S. Beutel, Flow rate dependent continuous hydrolysis of protein isolates, *AMB Express* 8 (2018) 18.
- M. de Cazes, M.P. Belleville, E. Petit, M. Llorca, S. Rodríguez-Mozaz, J. de Gunzburg, D. Barceló, J. Sanchez-Marcano, Design and optimization of an enzymatic membrane reactor for tetracycline degradation, *Catal. Today* 236 (2014) 146–152.
- G. Bayramoğlu, M. Yilmaz, M.Y. Arica, Immobilization of a thermostable α -amylase onto reactive membranes: kinetics characterization and application to continuous starch hydrolysis, *Food Chem.* 84 (2004) 591–599.
- S. Akgöl, G. Bayramoğlu, Y. Kacar, A. Denizli, M.Y. Arica, Poly(hydroxyethyl methacrylate-co-glycidyl methacrylate) reactive membrane utilised for cholesterol oxidase immobilisation, *Polym. Int.* 51 (2002) 1316–1322.
- T. Danisman, S. Tan, Y. Kacar, A. Ergene, Covalent immobilization of invertase on microporous pHEMA-GMA membrane, *Food Chem.* 85 (2004) 461–466.
- J. Hou, G. Dong, Y. Ye, V. Chen, Enzymatic degradation of bisphenol-A with immobilized laccase on TiO₂ sol-gel coated PVDF membrane, *J. Membr. Sci.* 469 (2014) 19–30.
- M.D. Hanwell, D.E. Curtis, D.C. Lonie, T. Vandermeersch, E. Zurek, G.R. Hutchison, Avogadro: an advanced semantic chemical editor, visualization, and analysis platform, *J. Cheminform.* 4 (2012) 17.
- S. Kroll, L. Treccani, K. Rezwan, G. Grathwohl, Development and characterisation of functionalised ceramic microtubes for bacteria filtration, *J. Membr. Sci.* 365 (2010) 447–455.
- J. Bartels, M.N. Souza, A. Schaper, P. Árki, S. Kroll, K. Rezwan, Amino-functionalized ceramic capillary membranes for controlled virus retention, *Environ. Sci. Technol.* 50 (2016) 1973–1981.
- V.B. Ivanov, J. Behnisch, A. Holländer, F. Mehdorn, H. Zimmermann, Determination of functional groups on polymer surfaces using Fluorescence Labelling, *Surf. Interface Anal.* 24 (1996) 257–262.
- M. Nyström, M. Lindström, E. Matthiasson, Streaming potential as a tool in the characterization of ultrafiltration membranes, *Colloid Polym. Sci.* 277 (1999) 297–312.
- P.K. Smith, R.I. Krohn, G.T. Hermanson, A.K. Mallia, F.H. Gartner, M.D. Provenzano, E.K. Fujimoto, N.M. Goeke, B.J. Olson, D.C. Klenk, Measurement of protein using bicinchoninic acid, *Anal. Biochem.* 150 (1985) 76–85.
- M.M. Bradford, A rapid and sensitive method for the quantitation of microgram quantities of protein utilizing the principle of protein-dye binding, *Anal. Biochem.* 72 (1976) 248–254.
- L. Visser, E.R. Blout, The use of p-nitrophenyl N-tert-butylloxycarbonyl-L-alanine as substrate for elastase, *Biochim. Biophys. Acta* 268 (1972) 257.
- D.J. Neidhart, G.A. Petsko, The refined crystal structure of subtilisin Carlsberg at 2.5 Å resolution, *Protein Eng.* 2 (1988) 271–276.
- T.J. Dolinsky, J.E. Nielsen, J.A. McCammon, N.A. Baker, PDB2PQR: an automated pipeline for the setup of Poisson-Boltzmann electrostatics calculations, *Nucleic Acids Res.* 32 (2004) W665–W667.
- D. Sitkoff, K.A. Sharp, B. Honig, Accurate calculation of hydration free energies using macroscopic solvent models, *J. Phys. Chem.* 98 (1994) 1978–1988.
- C.R. Søndergaard, M.H. Olsson, M. Rostkowski, J.H. Jensen, Improved treatment of ligands and coupling effects in empirical calculation and rationalization of pK_a values, *J. Chem. Theory Comput.* 7 (2011) 2284–2295.
- N.A. Baker, D. Sept, S. Joseph, M.J. Holst, J.A. McCammon, Electrostatics of nanosystems: application to microtubules and the ribosome, *Proc. Natl. Acad. Sci.* 98 (2001) 10037–10041.
- W. Humphrey, A. Dalke, K. Schulten, VMD: visual molecular dynamics, *J. Mol. Graph. Model.* 14 (1996) 33–38.
- B. Mueller, M. Zacharias, K. Rezwan, Bovine serum albumin and lysozyme adsorption on calcium phosphate particles, *Adv. Eng. Mater.* 12 (2010) B53–B61.
- F. Meder, H. Hintz, Y. Koehler, M.M. Schmidt, L. Treccani, R. Dringen, K. Rezwan, Adsorption and orientation of the physiological extracellular peptide glutathione disulfide on surface functionalized colloidal alumina particles, *J. Am. Chem. Soc.* 135 (2013) 6307–6316.
- J. Werner, B. Besser, C. Brandes, S. Kroll, K. Rezwan, Production of ceramic

- membranes with different pore sizes for virus retention, *J. Water Process Eng.* 4 (2014) 201–211.
- [44] J. Zhang, F. Ye, J. Sun, D. Jiang, M. Iwasa, Aqueous processing of fine ZrO₂ particles, *Colloids Surf. A Physicochem. Eng. Asp.* 254 (2005) 199–205.
- [45] R. Greenwood, K. Kendall, Selection of suitable dispersants for aqueous suspensions of zirconia and titania powders using acoustophoresis, *J. Eur. Ceram. Soc.* 19 (1999) 479–488.
- [46] R.A. Kimel, J.H. Adair, Aqueous degradation and chemical passivation of yttria-tetragonally-stabilized zirconia at 25°C, *J. Am. Ceram. Soc.* 85 (2002) 1403–1408.
- [47] F. Hussain, S. Arana-Peña, R. Morellon-Sterling, O. Barbosa, S.A. Braham, S. Kamal, R. Fernandez-Lafuente, Further stabilization of alcalase immobilized on glyoxyl supports: amination plus modification with glutaraldehyde, *Molecules* 23 (2018) 3188.
- [48] F. Meder, T. Daberkow, L. Treccani, M. Wilhelm, M. Schowalter, A. Rosenauer, L. Mädler, K. Rezwan, Protein adsorption on colloidal alumina particles functionalized with amino, carboxyl, sulfonate and phosphate groups, *Acta Biomater.* 8 (2012) 1221–1229.
- [49] K. Rezwan, L.P. Meier, L.J. Gauckler, Lysozyme and bovine serum albumin adsorption on uncoated silica and AlOOH-coated silica particles: the influence of positively and negatively charged oxide surface coatings, *Biomaterials* 26 (2005) 4351–4357.
- [50] M. Ottesen, I. Svendsen, *The Subtilisins*, G.E. Perlmann (Ed.), *Proteolytic Enzymes*, Academic Press, Inc., New York, 1970, pp. 199–215.
- [51] Z. Adamczyk, *Particles at interfaces - interactions, deposition, structure*, in: A.T. Hubbard (Ed.), *Interface Science and Technology*, Elsevier, London, 2017.
- [52] F.S. Markland, D.L. Smith, Subtilisins: primary structure, chemical and physical properties, in: P.D. Boyer (Ed.), *Hydrolysis: Peptide Bonds*, Academic Press, Inc., New York, 1971, pp. 561–608.
- [53] *Novozymes A/S, Enzymes for Biocatalysis*, Novozymes A/S, Bagsvaerd, 2016.
- [54] J.C. Cruz, P.H. Pfromm, J.M. Tomich, M.E. Rezac, Conformational changes and catalytic competency of hydrolases adsorbing on fumed silica nanoparticles: 1. Tertiary structure, *Colloids Surf. B Biointerfaces* 79 (2010) 97–104.
- [55] W. Huang, J. Wang, D. Bhattacharyya, L.G. Bachas, Improving the activity of immobilized subtilisin by site-specific attachment to surfaces, *Anal. Chem.* 69 (1997) 4601–4607.
- [56] P. Carter, J.A. Wells, Dissecting the catalytic triad of a serine protease, *Nature* 332 (1988) 564.
- [57] L. Polgár, The catalytic triad of serine peptidases, *Cell. Mol. Life Sci. CMLS* 62 (2005) 2161–2172.
- [58] P.W. Tardioli, J. Pedroche, R.L. Giordano, R. Fernández-Lafuente, J.M. Guisan, Hydrolysis of proteins by immobilized-stabilized alcalase-glyoxyl agarose, *Biotechnol. Prog.* 19 (2003) 352–360.
- [59] S. Ait Braham, F. Hussain, R. Morellon-Sterling, S. Kamal, J.F. Kornecki, O. Barbosa, D.E. Kati, R. Fernandez-Lafuente, Cooperativity of covalent attachment and ion exchange on alcalase immobilization using glutaraldehyde chemistry: enzyme stabilization and improved proteolytic activity, *Biotechnol. Prog.* 0 (2018).